Review

Predicting and Monitoring Cancer Treatment Response with Diffusion-Weighted MRI

CME

Harriet C. Thoeny, MD[1]* and Brian D. Ross, PhD[2]

An imaging biomarker that would provide for an early quantitative metric of clinical treatment response in cancer patients would provide for a paradigm shift in cancer care. Currently, nonimage based clinical outcome metrics include morphology, clinical, and laboratory parameters, however, these are obtained relatively late following treatment. Diffusion-weighted MRI (DW-MRI) holds promise for use as a cancer treatment response biomarker as it is sensitive to macromolecular and microstructural changes which can occur at the cellular level earlier than anatomical changes during therapy. Studies have shown that successful treatment of many tumor types can be detected using DW-MRI as an early increase in the apparent diffusion coefficient (ADC) values. Additionally, low pretreatment ADC values of various tumors are often predictive of better outcome. These capabilities, once validated, could provide for an important opportunity to individualize therapy thereby minimizing unnecessary systemic toxicity associated with ineffective therapies with the additional advantage of improving overall patient health care and associated costs. In this report, we provide a brief technical overview of DW-MRI acquisition protocols, quantitative image analysis approaches and review studies which have implemented DW-MRI for the purpose of early prediction of cancer treatment response.

Key Words: diffusion-weighted MRI; oncology; treatment monitoring; biomarker
J. Magn. Reson. Imaging 2010;32:2–16.

PATIENTS SUFFERING FROM a malignant tumor or metastases undergo extensive therapies including various side effects. Up to date treatment response is evaluated by morphological, clinical, and laboratory outcome. Radiological tumor response is based on the extent of tumor size reduction as measured by anatomical imaging modalities such as computed tomography (CT) or MRI. However, therapy is typically delivered in fractionated doses, thus requiring sufficient time for enough treatment to be delivered to kill cells within the tumor as well as additional time needed for immunological removal of the macromolecular debris. Thus, therapy-induced changes in tumor volumes often occur relatively late in the time course of treatment.

Current therapeutic strategies in oncology include surgery, radiation therapy, and chemotherapy, which includes molecularly targeted agents against oncogenic signaling pathways as well as vascular targets. However, timely evaluation of treatment response in patients undergoing radiation therapy or chemotherapy, depending on the underlying pathology or treatment strategy, is often very difficult. Evaluation of the response to chemotherapy, based on changes in the size of solid tumors, is typically evaluable after 6 to 8 weeks.

Development of antiangiogenic agents, and vascular and molecularly targeted agents may not lead to significant reduction in tumor size. Antiangiogenic agents inhibit neovascularization of tumors, and vascular targeting agents selectively destroy pathological vessels without interfering with normal vessels. Molecularly targeted agents for example, are directed at oncogenic signaling molecules, which can for example lead to a variety of biological effects including inhibition of growth or apoptotic-induced cell death. In 2000, RECIST (response evaluation criteria in solid tumors) defined the response to treatment in terms of alteration of tumor size only (1). However, as newer agents might provide therapeutic benefit by other mechanisms than size reduction, new evaluation criteria are of utmost importance. Recently, these RECIST criteria were reconsidered and are considering imaging biomarkers such as positron emission

[1]Department of Radiology, University Hospital of Bern, Inselspital, Bern, Switzerland.
[2]Departments of Radiology and Biological Chemistry, The University of Michigan Medical School, Ann Arbor, Michigan, USA.
Contract grant sponsor: Swiss National Science Foundation for Scientific Research; Contract grant number: 320000-113512; Contract grant sponsors: Carigest SA Foundation, Geneva, Switzerland; National Institutes of Health; Contract grant numbers: P50CA093990, P01CA085878.
*Address reprint requests to: H.C.T., University Hospital of Bern Inselspital, Department of Diagnostic, Pediatric and Interventional Radiology, Freiburgstrasse 10, 3010 Bern, Switzerland.
E-mail: harriet.thoeny@insel.ch
Received August 26, 2009; Accepted February 19, 2010.
DOI 10.1002/jmri.22167
Published online 14 May 2010 in Wiley InterScience (www.interscience.wiley.com).

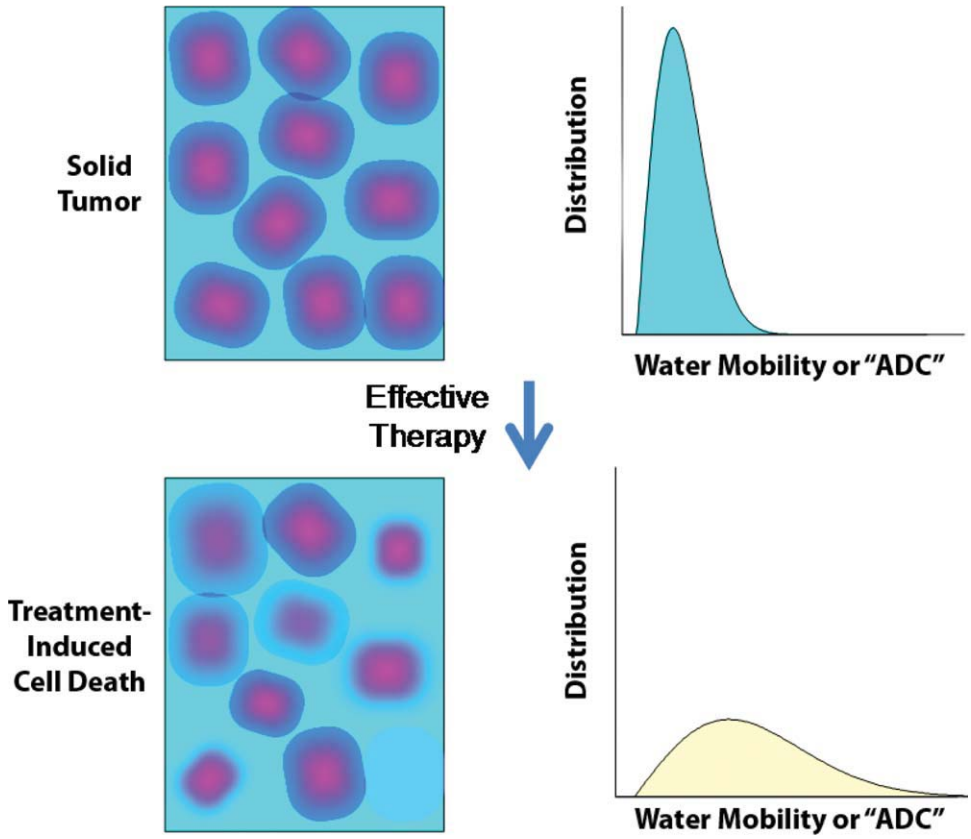

Figure 1. Schematic representation of the relationship between change in cellular density following an effective therapy and the corresponding distribution of water diffusion values within the tumor. Note that the mean diffusion value of a tumor increases early following the loss of cellular density. [Color figure can be viewed in the online issue, which is available at www.interscience.wiley.com.]

tomography (PET) (2). In these articles, it has already been considered that the up to date anatomic unidimensional assessment of tumor burden has to be changed to volumetric anatomical assessment as well as functional assessment including PET and MRI.

Clinical assessment of new treatments in oncology is evaluated by numerous response criteria, including tissue and plasma biomarker readouts, improvement in quality of life, and survival among others. As the process to quantify response of agents undergoing clinical trials may be lengthy, there is a significant need for timelier outcome measures to be identified and validated. The ability to quantify the effectiveness of experimental therapies would significantly impact the overall drug development process and offers the potential of using DW-MRI to provide for early evaluation and go, no-go decisions in phase 1 clinical trials thus saving money and time. Thus early surrogate indicators that correlate with long-term outcome metrics are urgently needed (3). Clinical trial measures that could provide early readouts of drug-target interactions and subsequent efficacy would facilitate quantification of outcomes in clinical trials and ultimately provide assistance in the regulatory approval process.

The current functional methods for response assessment as suggested by RECIST 1.1 includes PET, PET-CT, magnetic resonance spectroscopy as well as dynamic contrast enhanced MRI. PET and PET-CT are quite expensive methods and the differentiation between residual tumor and inflammation is often quite difficult using tracers such as [F18]fluorodeoxyglucose. Furthermore, radiation exposure is a drawback mainly in younger patients undergoing several follow-up studies for response assessment. MR spectroscopy is a very promising method; however, its limitations include low spatial resolution, restricted availability and lack of expertise of many radiologists. Dynamic contrast enhanced MRI provides information on changes in vascularization of the tumor during treatment; however, image analysis is relatively complicated and, therefore, not suited for daily clinical routine. Furthermore, the risk of nephrogenic systemic fibrosis—although being very small—has to be taken into account in patients with renal insufficiency.

Diffusion-weighted MRI (DW-MRI) has not been considered in RECIST 1.1; however, this noninvasive MR technique has been discussed as cancer biomarker in a consensus meeting at the ISMRM 2008 and a publication on consensus and recommendations for DW-MRI as a cancer biomarker has been published recently highlighting the potential of this promising technique in cancer patients (4).

DW-MRI for the evaluation of early treatment response is very promising. As diffusion within tumors is impeded by the presence of cellular membranes and macromolecular structures, treatment with for example radiation and/or chemotherapy can result in the loss of cell membrane integrity, which can be detected as an increase in mean diffusion value for the tumor as shown in Figure 1. Thus, DW-MRI can provide microstructural information on the cellular level. Animal and clinical studies to date have

revealed that successful treatments of a wide variety of tumor types can be detected as an increase in tumor ADC values due to the loss of cellular density.

TECHNICAL REQUIREMENTS

Several technical requirements to perform follow-up of cancer patients using DW-MRI have to be considered. Standardized techniques including patient preparation for follow-up scans are important, e.g., when evaluating the pelvis the filling of the urinary bladder has to be taken into consideration. Parallel imaging techniques offer several advantages for DWI, particularly at high magnetic fields where magnetic field inhomogeneity leads to large spatial distortion when using single-shot EPI. Parallel imaging techniques use previously acquired receiver coil sensitivity patterns to reduce the quantity of phase-encode lines required to reconstruct an image (5–7). This allows a shorter single-shot echo train interval, thereby reducing inhomogeneity-induced phase accumulation manifest as geometric distortion. There is a signal-to-noise ratio (SNR) penalty associated with collecting fewer phase-encode lines, but it can be offset by the SNR gain achieved by the reduced minimum echo time afforded by parallel imaging. Furthermore on the negative side, parallel imaging may introduce artifacts characterized by nonuniform noise and wrap-like artifacts that occur at spurious locations within the field-of-view. However, usually the benefits of parallel imaging methods outweigh the drawbacks when applied to single-shot EPI-based DW-MRI of the body. Therefore, incorporation and trial of parallel imaging in these protocols is encouraged, especially on 3 Tesla (T) systems.

There are several options to reduce respiratory motion artifacts when performing DW-MRI of the chest and abdomen. When performing DW-MRI with free breathing, multiple averaging is necessary to increase SNR and reduce respiratory effects, although this can lead to partial volume averaging and blur of internal structures (8). Breathhold images are another option, however, in cancer patients free breathing is often easier to perform in severely ill individuals. Even if the patient is able to hold his or her breath, signal averaging within the breathhold interval is severely limited, leading to low SNR. At the expense of increased scan time, respiratory triggering or cardiac gating may be used when performing DW-MRI in the chest or upper abdomen. Although in a recent analysis of motion control techniques it was noted that respiratory-triggering yielded significantly higher ADCs and lower ADC reproducibility than breath hold or nonbreathhold scans (9,10). Anti-peristaltic agents can be administered mainly when examining the lower abdomen and the pelvis to avoid or minimize bowel motion artifacts.

DW-MRI is usually performed in the three orthogonal diffusion directions to minimize the influence of anisotropy, although the degree of diffusion anisotropy in non-neural tissues and tumor is relatively low. By acquisition of DW-MRI in three orthogonal directions, a rotationally invariant diffusion coefficient can be calculated, that is, the diffusion measurement is independent of the relative orientation of the tissue architecture and gradient axes. Optimization of fat suppression should also be considered. Presence of fat signal in single-shot EPI DW-MRI is particularly problematic because the apparent location of fat structures are displaced many pixels along the phase-encode direction thus may superimpose water-based signals. This not only obscures the tissues of interest, but also greatly distorts ADC measurement because lipid protons have a very low diffusion coefficient. Standard fat suppression techniques are applicable to DW-MRI and include frequency-selection saturation of fat signal, use of adiabatic pulses to reduce sensitivity to B1 inhomogeneity in frequency-selection saturation/inversion of fat, and nonfrequency selective Short TI Inversion Recovery (STIR) methods that are less affected by poor shim quality (11–13).

DW-MR images at a minimum of two sensitivity levels defined by the sequence b-value must be acquired to quantify ADC. Proper selection of b-values depend on the given body DW-MRI application and objective. The majority of clinical neuroimaging DWI studies have been performed at b = 0 and 1000 s/mm^2 and has grown acceptance as the default b-value set for brain DW-MRI. However, microcirculation through randomly oriented capillaries in the presence of diffusion-sensitization gradients will also appear as a hyper diffusion-like attenuation particularly in the low b-value regimen (i.e., b = 0 to 100 s/mm^2). Certainly perfusion must be considered fundamentally distinct from thermally driven diffusion, but perfusion effects can be observed in DW-MRI particularly in vascular-rich tissues/lesions thus should be considered in design of DW-MRI protocols. Therefore, if one seeks to disentangle perfusion effects from molecular diffusion, additional b-values are required in the low b-value range (0–100 s/mm^2), which are sensitive to perfusion effects, for contrast against nominal high b-value decay, which is dominated by diffusion. The y-intercept extrapolated from fitting signal decay versus b-value using intermediate to high b-values compared with the b = 0 s/mm^2 signal can be used as an estimate of the perfusion signal component. Therefore, collection of the b = 0 DW-MRI (i.e., T2-weighted image) is valuable to elucidate perfusion and diffusion influences. Figure 2 illustrates this perfusion effect in human kidney. Diffusion estimates are derived from the exponential decay of DW-MRI signal versus b-value. If a simple two-point estimate of signal decay is used (as often is the case), then:

$$S(b) = S_o e^{-Db} \quad or \quad D = \frac{1}{(b_2 - b_1)} \ln\left[\frac{S(b_1)}{S(b_2)}\right] \qquad [1]$$

where b_1 and b_2 represent the low and high b-values. By estimating ADC by means of the slope of log(signal) versus b-value using b-values > 100 s/mm^2, most of the perfusion signal is attenuated leading to an ADC estimate relatively free of perfusion contamination. At high b-values, however, the signal may falsely exhibit a multi-exponential shape due to the signal falling

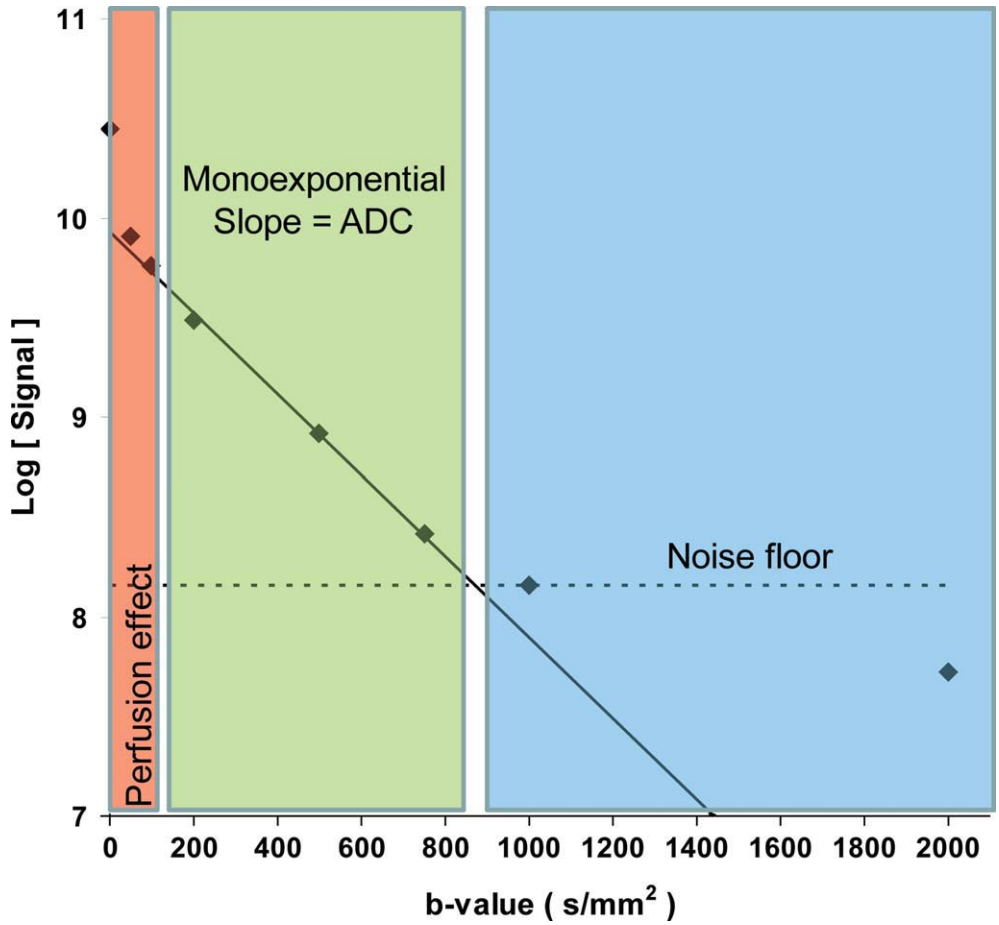

Figure 2. Measured signal decay in kidney cortex of as a function of b-value. Perfusion effect is dominant in the low b-value range (0–100 s/mm^2) and would inflate ADC if included in slope calculations. By extinguishing most of the vascular signal at b values greater than 100 s/mm^2, a true estimate of ADC is derived. Using b-values 100 to 750 s/mm^2, the estimated kidney ADC = 2.03 $\times$ 10^{-3} mm^2/s. The dashed line represents the noise floor. DW-MRI measurements where signal falls within the noise floor lead to erroneous ADC estimates and a false multi-exponential appearance to the log(signal) versus b-value curve. Tissues do exhibit true multi-exponential diffusion decays over a wide b-value range (b = 500 to > 3000 s/mm^2), although very high SNR is required to document these features. [Color figure can be viewed in the online issue, which is available at www.interscience.wiley.com.]

beyond the noise floor (see Fig. 2 for b = 1000 to 2000 s/mm^2). The maximum b-value should be set such that signals recorded at that b-value are adequately above the noise floor. This maximum b-value depends on the SNR achievable for the target organ/tissue and the water diffusion coefficient of these tissues—the lower the diffusion value, the higher the b-value achieved before the signal approaches the noise floor. Tissues do exhibit true multi-exponential diffusion decays over a wide b-value range (b = 500 to > 3000 s/mm^2), although very high SNR is required to document these features (14).

IMAGE ANALYSIS

To evaluate DW-MRI, there are two general categories for image analysis: qualitative and quantitative. Moreover, the "image" may represent several quantities derived from DW-MR images. For example, ADC maps may be calculated over a specified b-value range, the image may represent an anisotropy index derived from a series of multiple directions of DW-MR images, or the image may represent an index that quantifies the multiexponential features of the diffusion decay over a wide range of b-values.

Shown in Figure 3 are a series of liver images acquired with varying b-values of 0, 100 and 600 s/mm^2. Note the heavily T2-weighted contrast at b-value of 0 s/mm^2 which includes bright vascular signal. The vascular signal is greatly attenuated at moderate diffusion weighting of 100 and 600 s/mm^2. Calculated ADC maps derived from the low b-value data (0 and 600 s/mm^2) yield ADC maps highly influenced by flowing blood. Use of moderate to high b-values (b = 100 to 600 s/mm^2) provide a more accurate measure of water diffusion free of vascular contamination (Fig. 3).

In general, water diffusion in tissue may be anisotropic; that is directionally dependent on the natural underlying directionality of cellular elements that impede water mobility. Neural tissue in particular is highly anisotropic where the diffusion coefficient may vary several-fold dependent on the relative orientation of the diffusion encoding gradient and the tissue structure. Most non-neural tissue exhibit nearly

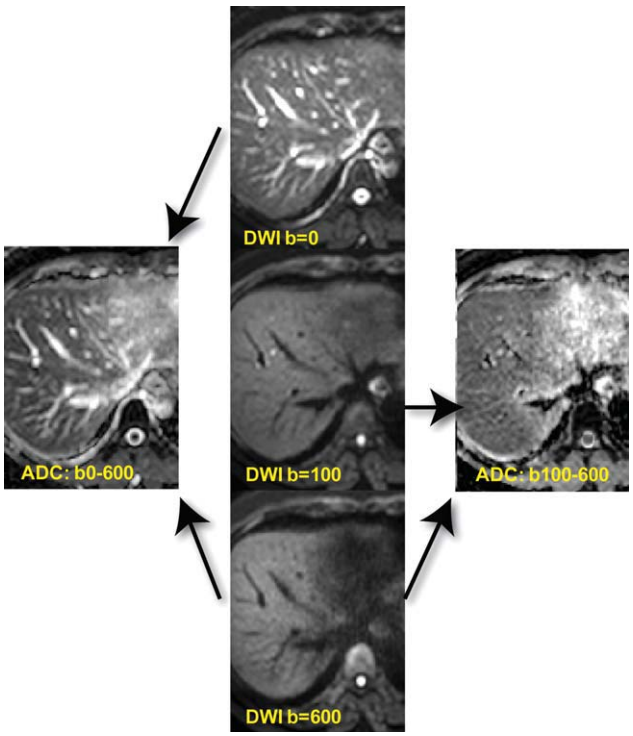

Figure 3. Effects of b-values on blood flow contribution to images and ADC maps. DW-MRI of the liver with b-values of 0, 100, and 600 s/mm^2 (center column) revealing suppression of vascular signal with increasing b-value. ADC maps generated using b-value images of 0 and 600 s/mm^2 as well as 100 and 600 s/mm^2. ADC maps generated using b-values of 100 and 600 s/mm^2 have attenuated contribution/contamination from perfusion effects (right ADC map) compared with the ADC map generated using b-values of 0 and 600 s/mm^2. [Color figure can be viewed in the online issue, which is available at www.interscience.wiley.com.]

isotropic water diffusion; although in general one should not assume tissue is isotropic when performing diffusion measurements. Diffusion encoding should be performed along at least three orthogonal gradient directions to properly account for possible anisotropy.

QUALITATIVE ASSESSMENT

The signal intensity change during treatment can be assessed by visual analysis of the underlying pathology as shown in Figure 4. In this example of a patient with two distinct hepatocellular carcinomas treated with transarterial chemoembolization (TACE), the solid tumors before treatment on a high b-value image show high signal intensity while the corresponding ADC maps exhibit low signal intensity. During successful treatment, the loss of cellularity in the upper tumor resulted in the high b-value image to shift toward lower signal intensity or high signal intensity on the corresponding ADC map. Although these are early changes, formation of fibrosis in the extracellular matrix can also occur later on during therapy and in some types of tumors if this occurs, it would result in low signal intensity on the high b-value image and on the corresponding ADC map. Posttherapeutic changes such as edema during radiation therapy demonstrate high signal intensity on the high b-value image as well as on the corresponding ADC map. An additional issue arising when using b-images as the singular image to base disease or treatment response assessment is the "T2 shine-through" effect. This effect can result in a tissue region appearing to exhibit higher signal intensity on b-images in the range of 500–1000 s/m^2 due to complicating factors such as the long intrinsic T2-relaxation time of the tissue. Avoidance of mis-interpretation of images due to artifactual T2-shine through effects can be accomplished by comparison with the corresponding ADC map.

QUANTITATIVE ASSESSMENT

In general, advancement of a biomarker must be demonstrated in multicenter trials with standardized acquisition techniques and with appropriate quality control (QC) standards to provide quantitative agreement across systems and assess overall repeatability. These quality issues require investigators to agree upon an appropriate QC phantom. A specific phantom for this purpose has not been decided upon by the broader community, although phantoms for DW-MRI have been proposed (15,16). Recent consensus has been reached as to a variety of issues by a consortium of investigators brought together by the National Institutes of Health to form overall recommendations (4).

Quantification of diffusion properties as a potential early surrogate response metric of clinical efficacy is commonly accomplished. There are two primary approaches to perform quantitative analysis of DW-MRI derived maps: (i) change in mean ADC value over the entire tumor or select spatial zones of the tumor, and (ii) a voxel-by-voxel change in ADC maps or other diffusion parametric maps.

In oncologic imaging applications, these two areas are particularly noteworthy to assess treatment response. The two distinct approaches involved in quantitative analyses of tumor ADC changes mentioned above are highlighted in the discussion below.

CHANGE IN ADC FOLLOWING THERAPY

This is a simple method that uses the whole tumor average ADC value where an increase in ADC following therapy due to a decrease in cellularity suggests a positive therapeutic response (Fig. 1) (17,18). This approach has been widely used in animal tumor studies where tumor treatments are very effective and tumor cell lines tend to be more responsive to interventions and in a shorter time span than is observed clinically (17,19–30). Moreover, extracting ADC values from ADC maps by drawing regions of interest around the margin of the tumor is relatively simple to perform. The resultant distribution of ADC values are typically plotted in a histogram format and the mean or median value is used to evaluate changes following treatment over time. However, histogram-based detection of treatment-induced diffusion changes can be attenuated if spatially varying diffusion values occur

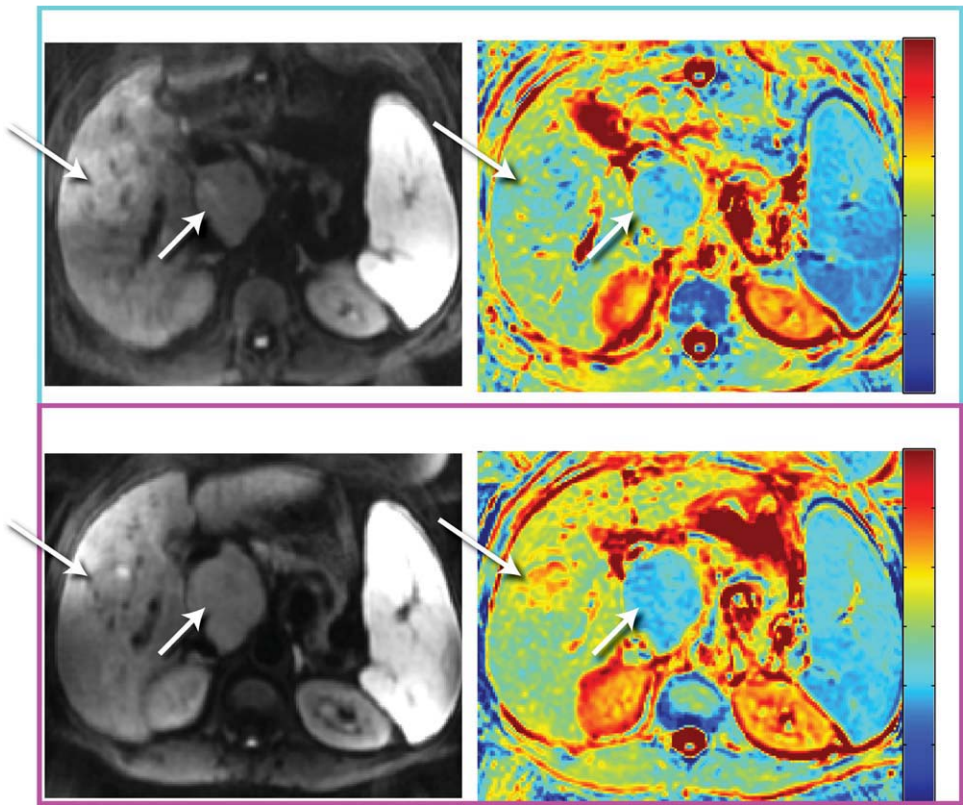

Figure 4. A patient with a hepatocellular carcinoma in the liver undergoing treatment with transcatheter arterial chemoembolization (TACE) (top row) pre and (bottom row) posttherapy. Each set of images consists of the DW-MRI (left images) along with their corresponding color ADC overlay maps (right column).

wherein both an increase and a decrease occur within the tumor. In this situation, competing factors would reduce the mean shift in ADC using a histogram-based approach. Furthermore, if large cystic or necrotic regions are present within the tumor mass, these would also have the potential to reduce detectable changes in tumor ADC values following treatment as they would "weight" the number of unchanged values according to their proportion of the total voxels thus reducing the overall net change in ADC value. Therefore, the histogram-based approach for detection of treatment response can be attenuated by pre- and posttreatment spatial heterogeneity within the tumor.

PARAMETRIC RESPONSE MAP ANALYSIS

In an effort to address the effects of spatial heterogeneity within the tumor mass, a voxel-by-voxel approach was proposed (31). This voxel-based approach spatially registered the pretreatment ADC map to a posttreatment initiation ADC map to provide for quantification of diffusion changes on the voxel level. Using this approach, changes in individual voxels can be tested for significance and superimposed on anatomic maps to reveal the spatial information within the context of the three-dimensional view of the tumor. ADC changes are encoded as color maps and overlaid on the anatomical MRI to obtain spatial information. This approach provides for the possibility of also guiding the therapist in adapting therapy early as well as assisting in the ability to spatially guide a directed therapy approach. The voxel-based analytical method was termed the functional diffusion map (fDM) and more recently the parametric response map (PRM) as it allows for quantification of the relative area or percentage of tumor volume in which significant change had occurred as the response metric (either a decrease or increase in ADC values) (Fig. 5). Shown in Figure 5, changes in tumor cellular structures can occur due to an apoptotic cell death process, which would result in the decrease in tumor cellularity thus causing an increase in tumor ADC values in those regions. Swelling of tumor cells would produce a drop in ADC values transiently, which upon conversion to necrosis, would produce an elevated ADC value. Image registration of pretreatment ADC maps with a follow up ADC map acquired following treatment initiation allows for presentation of the PRM_{ADC} data both in terms of a three-color overlay where red indicates increased ADC values, blue decreased ADC values and green unchanged ADC values as shown in Figure 5. These data can also be shown as a scatter plot and quantification of changes presented as a percent of tumor voxels (i.e., volume) with increased ADC values (Fig. 5). This technique is readily applied in tumor sites where tumor growth is modest and tumors can be spatially registered with well established algorithms such as the affine transform. Extension of PRM to monitoring of tumors located at other sites where tumor growth and/or surrounding tissues are more elastic can be implemented using nonlinear warping algorithms for image registration (32).

Applications of PRM_{ADC} tumor treatment response monitoring have been reported in both animal and clinical studies. Correlation of increased PRM values following treatment in a brain tumor glioma model

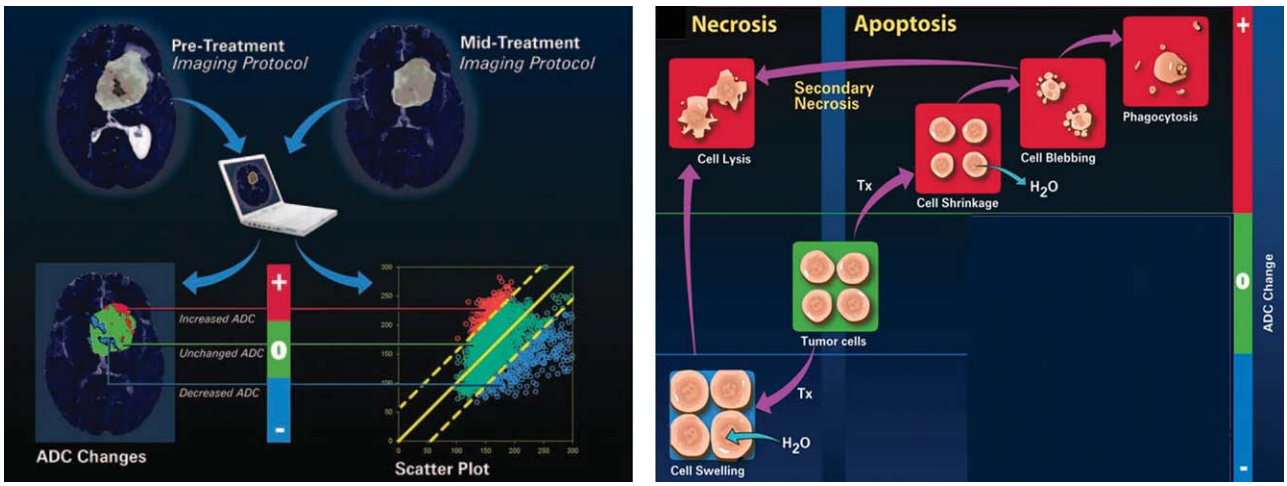

Figure 5. (Left panel) Diagrammatic representation of two possible pathways of cell death associated with therapy. Induction of apoptosis which would lead to an increase in tumor ADC values due to cell shrinkage and loss of cellular density. Processes involved with the induction of necrosis which might exhibit a transient initial drop in ADC values due to cell swelling following by an increase in ADC values during cell lysis during the later stages of this death pathway. (Right panel) The voxel-by-voxel analytical approach (functional diffusion map [fDM] or parametric response map [PRM_{ADC}]) used to quantify diffusion changes following therapy within a tumor using ADC maps pre- and posttreatment initiation. (Used with permission. Moffat BA, Chenevert TL, Lawrence TS, et al. Functional diffusion map: a noninvasive MRI biomarker for early stratification of clinical brain tumor response. Proc Natl Acad Sci USA 2005;102:5524–5529. Copyright (2005) National Academy of Sciences, USA).

revealed that measurement of early changes at 4 days after treatment of the PRM_{ADC} metric correlated with overall survival in a dose-response chemotherapy study (33). This animal study validated the PRM imaging biomarker as an early response predictor for animal studies. Several clinical studies have also been reported in grade III/IV glioma patients (31,34,35) and in head and neck tumor patients (32). Overall, these clinical studies have reported correlation of early PRM_{ADC} changes with late, traditional clinical outcome measures revealing the potential utility of this voxel-based approach as an imaging oncologic response biomarker. Finally, extension of the voxel-by-voxel analysis approach has been reported using MRI perfusion maps from brain tumor patients undergoing therapy wherein changes as early as 1 week into therapy could be used to predict patient outcome (36). This study reveals that the voxel-by-voxel approach may provide improved sensitivity for treatment response assessment for a broad range of imaging modalities which includes DW-MRI.

MULTIEXPONENTIAL DIFFUSION/PERFUSION PROPERTIES OF TREATED TUMORS

The signal loss in DW-MRI with increasing b-value does not necessarily follow a monoexponential decay (37). The perfusion component of tissue appears as a "hyper diffusion-like" decay with b-value over the low b-value regimen (0–100 s/mm^2). At higher b-values (>100 s/mm^2), the perfusion signal is largely extinguished, thus, ADC measurements are more heavily influenced by the water diffusion properties within the cellular matrix. The apparent diffusion coefficient provides us information on diffusion and perfusion provided that these two entities can be separated.

In an experimental study in rats, DW-MRI was performed for monitoring the effect of a vascular targeting agent on rhabdomyosarcomas (38). As vascular targeting agents selectively destroy pathological vessels the aim of the study was to perform DW-MRI to detect changes in diffusion and perfusion noninvasively and without contrast medium administration. For that reason, three different ADC values were calculated out of a large series of b-values: to approximate true diffusion an ADC was calculated only out of high b-values (500, 750, 1000 s/mm^2 = ADC_{high}). An ADC including b-values from 0 to 100 s/mm^2 (perfusion and diffusion) was considered as ADC_{low}, whereas the difference between ADC_{low} and ADC_{high} was hypothesized to approximate perfusion. In addition, when ADC is used, it is assumed to mean from values generated using b-values between 0 and 1000 s/m^2.

In this study performed on rhabdomyosarcomas in rats, imaging was performed before administration of this vascular targeting agent, 1 h, 6 h, 2 days, and 9 days after start of therapy, where morphological images, including images before and after contrast medium administration as well as DW-MR images were performed during treatment and histopathological correlation at each time point were presented (38).

One hour after vascular targeting injection leading to disruption of the pathological vessels, no perfusion of the solid tumor could be detected. However, the corresponding ADC map still showed vital tumor cells reflected as a low signal intensity of the solid tumor confirmed by histology. Similar findings were observed 6 h after injection of the vascular targeting

agents. The reason for the lack of enhancement as seen on conventional postcontrast T1-weighted fat saturated images was determined to be vasoconstriction and vasocongestion, which was identified on histological tumor sections. Only 2 days after therapy, the morphological images showing necrosis corresponded to tumor death on the ADC map, which was also confirmed histologically. Nine days after treatment, the tumor started regrowing from the periphery as seen on morphological images, the same results were also seen on ADC maps and corresponding histological specimens.

When measuring the ADC values early after treatment (1 and 6 h), a decrease in ADC_{high} was seen and attributed to cell swelling and consequent impeded diffusion in the extravascular space. The decrease in perfusion was due to vascular shutdown. During true necrosis at 2 days, the ADC_{high} increased, whereas ADC_{high} during relapse decreased again due to increase in cellularity of the tumor. In another study, the difference between ADC_{low} and ADC_{high} as suggested corresponding to perfusion was correlated with the volume transfer constant k calculated from dynamic contrast enhanced images during follow-up of treatment. A correlation between these two parameters calculated from these two different techniques was demonstrated, suggesting that dynamic contrast enhanced MRI provided information on perfusion changes during treatment, whereas DW-MRI was able to provide information on perfusion changes and also allowed for differentiation between viable and necrotic regions within the tumor mass (39).

As it has already been suggested by Le Bihan, separation of diffusion and perfusion in intravoxel incoherent motion MR imaging should be performed and this was reconsidered in a recent paper published in *Radiology* from the same author (40). As many treatment strategies lead to changes on different levels of the tumor, the differentiation between diffusion and perfusion calculated from the DW-MR images might help to provide information on additional and more subtle changes that might occur during treatment.

DW-MRI AS BIOMARKER

DW-MRI as biomarker has several advantages because it provides microstructural changes related to treatment effects over time that usually precede change in size. No ionizing radiation and no injection of isotope or any other contrast medium is necessary. Furthermore, the acquisition time to perform DW-MRI lasts only a few minutes, the method is easily repeatable providing quantitative information and information on spatial distribution including heterogeneity of the tumor and its response. In addition, this technique is magnetic field independent and, therefore, multicenter and longitudinal studies can be performed easily.

Early detection of treatment response might change therapeutic strategies in case of nonresponders to avoid toxicity and other negative side effects; it might allow individualizing treatment and hopefully increase long-term survival. In addition, money for ineffective treatment can be saved. DW-MRI in oncology has several key applications including diagnosis, tumor staging, and early evaluation of treatment response and detection of relapse.

DW-MRI for monitoring therapy has already been applied in a wide variety of cancer types and organ sites, including the liver, breast, bone, soft tissue tumors, cervical tumors, head and neck tumors, as well as rectal cancer (41–65).

CLINICAL APPLICATIONS OF DW-MRI FOR MONITORING TREATMENT RESPONSE IN DIFFERENT ORGAN SITES

Liver Metastases

Hepatic metastases are the most common neoplasms in the liver. Only selected lesions can be surgically resected, therefore, the vast majority of tumors are treated by chemotherapy. Size reduction as ultimate response to successful treatment often occurs relatively late; hence, early detection of response based on DW-MRI findings would be helpful to avoid unnecessary treatment in case of therapy failure. Several articles already showed that systemic chemotherapy of liver metastases had a good correlation of response with increased ADC values following treatment (28,47,48).

In a study that has been performed in 2004 in patients with liver metastases from breast cancer, a correlation between ADC changes and tumor reduction was found at 4 and 11 days after start of therapy. The authors concluded that DW-MRI could be used to predict the response of liver metastases to effective chemotherapy (28). Similar results were reported in a study of 20 patients with potential operable hepatic lesions larger than 1 cm in diameter metastatic from colorectal carcinoma. In this study, quantitative ADC maps were calculated separately with b-values from 0 to 500 and with b-values from 150 to 500 s/mm^2. The nonresponding lesions had a significantly higher pretreatment mean ADC (ADC 0–500 and mean ADC 150–500) than did responding lesions. After chemotherapy, responding lesions had a significant increase in ADC, whereas no significant change was observed in nonresponding metastatic lesions after chemotherapy (47). The authors conclude that high pretreatment mean ADC values of liver metastases from colorectal cancer were predictive of poor response to chemotherapy. Responding lesions showed a significant increase in mean ADC in contrast to nonresponding lesions, indicating the potential of this method for the development of individualized therapy. These results were confirmed by a recent study performing DW-MRI as a potential imaging biomarker for prediction and early detection of response to chemotherapy in a total of 87 liver metastases (from colorectal and gastric carcinomas). The pretreatment mean ADCs5 in responding lesions were significantly lower than those of nonresponding lesions ($P = 0.003$). An early increase in ADC (on day 3 and 7) was observed in responding lesions in contrast to nonresponding lesions ($P = 0.002$),

preceding the effects of change in size that was only possible at a later time point. The authors concluded that ADC seems to be a promising tool for helping to predict and monitor the early response to chemotherapy of hepatic metastases from colorectal and gastric carcinomas (48).

In 12 patients with 48 metastatic liver lesions from colorectal cancer, DW-MRI was applied for the evaluation of therapeutic response to hepatic arterial infusion chemotherapy (HAIC) with 5-fluorouracil (49). Imaging was performed before and 9 days after HAIC. Positive correlations were observed for relative change between %min ADC and reduction ratio ($r = 0.709$) and between %mean ADC and reduction ratio ($r = 0.536$). Both parameters (%min ADC and %mean ADC) were significantly greater in the responder group than in the nonresponder group as evaluated on follow-up CT after 3 months. These results show the usefulness of DW-MRI for early detection of response of liver metastases undergoing treatment with HAIC.

Malignant Liver Lesions

In recent years interventional techniques such as TACE and hepatic radiofrequency (RF) ablation gained importance in the curative or palliative treatment of hepatocellular carcinoma (HCC) or of liver metastases. The early assessment of successful treatment or relapse is important in patient management; however, the differentiation between residual or recurrent tumor from nontumoral tissue changes following thermotherapy or chemoembolization is a challenging issue when applying conventional techniques including CT or MRI.

Navigator respiratory-triggered DW-MRI in the follow-up of hepatic RF ablation in 54 patients with 77 liver lesions (17 primary tumors, 60 metastases due to different underlying tumors in 37 patients) showed promising results in the detection of local tumor progression compared with nontumoral posttreatment tissue changes (50). Hyperintensities in the periphery of the ablation zone of the tumor on DW-MR images on 58 of 148 examinations corresponded to local tumor progression confirmed by follow-up in only 17 of these lesions, whereas the remaining signal alterations disappeared during follow-up. However, when performing quantitative analysis of these suspicious hyperintense areas on the corresponding ADC map the ADC values were significantly lower in case of local tumor progression than in cases without tumor progression (102.1 ± 22.4 versus $130.8 \pm 47.6 \times 10^{-5}$ mm^2/s; $P = 0.00124$), suggesting the potential of DW-MRI in this particular setting.

In 24 patients with unresectable HCC undergoing TACE, contrast-enhanced MRI and DW-MRI were performed before, 24 h, and 1, 2, 3, and 4 weeks after therapy (51). Mean tumor size was unchanged up to 4 weeks after TACE, whereas reduction in tumor enhancement in the arterial and portal venous phase occurred immediately after therapy with a consistent reduction in the first 3 weeks. The increase in tumor ADC value was significant 1–2 weeks after therapy ($P = 0.004$), borderline significant after 3 weeks, and insignificant after 24 h and 4 weeks after therapy. In another study in 23 patients with 26 HCCs treated with TACE, DW-MRI improved the sensitivity of DCE-MRI (85% to 92%) in the detection of peri-lesional tumor recurrence; however, its specificity decreased from 65% to 50% after adding DW-MRI (52). In this study, b-values of 50, 400, and 800 s/mm^2 were applied. As biexponential fitting provides more detailed information on perfusion and diffusion changes separately, this technique might be helpful in this particular setting were perfusion changes are expected to appear; however, this can only be done on the expense of longer imaging times.

Overall the utility of DW-MRI for monitoring treatment response in HCC and metastases is very promising and may provide the possibility of individualizing treatments for this population of patients.

Pancreatic Cancer

As pancreatic cancer is often diagnosed at an advanced stage, a curative surgical approach is often too late and chemotherapy or chemoradiotherapy are the only treatment options. The stratification of responders and nonresponders at an early stage after initiation of treatment might allow to change or stop therapy avoiding the high risk of complications and side effects and ultimately save unnecessary expenses for useless treatments.

In a recent study, a consecutive group of 63 patients with advanced pancreatic cancer who were treated with chemotherapy underwent DW-MRI before therapy and follow-up was performed by CT (53). The patients were classified into two groups according to the findings during follow-up: (a) those with progressive disease and (b) those with stable disease at 3 and 6 months after initial treatment. DW-MRI was applied using three b-values (0, 400, and 1000 s/mm^2), and a middle (including a b-value of 400 s/mm^2) and high (including a b-value of 1000 s/mm^2) ADC were calculated in the solid parts of the tumor. The results of this study showed that the rate of tumor progression was significantly higher in those with a lower high b-value ADC than in those with a higher b-value ADC. The authors concluded that a lower high b-value ADC in patients with advanced pancreatic carcinoma may be predictive of early progression in chemotherapy-treated patients. Of interest, these findings are contradictory to liver metastases where a low pretreatment ADC value was correlated with better outcome after treatment (47,48), however, similar to findings reported in rectal cancer (43,54). In pancreatic cancers, a low ADC corresponding to early progression might be attributed to a high cellularity with consequent higher aggressiveness of the tumor but due to the worse response might probably be related to desmoplastic reaction in the tumor before treatment.

Breast Cancer

Neoadjuvant chemotherapy in patients with breast cancer is a relatively controversial issue; however, this treatment is helpful to reduce size of the tumor before

surgery with a consequent improved rate for breast conserving surgery. DW-MRI is ideal for monitoring treatment response, because the results can be correlated with histology. In responding primary breast cancers, increased ADC values have been reported. Changes in ADC after the first cycle of chemotherapy significantly correlated with volume and diameter (42,55). The pretreatment ADC values in a study including a control group, the contralateral normal breast as well as benign lesions and malignant lesions before therapy, were lowest in the malignant breast lesions compared with all the other groups. A change in ADC after the first cycle was statistically significant compared with volume and diameter at the end of treatment indicating the potential in assessing early response. It has been concluded, that the results of this study show that the ADC is more useful for predicting early tumor response to new adjuvant chemotherapy than morphological variables suggesting its potential in effective treatment management (42).

In a breast cancer human xenograft model treated with chemotherapy, the mean change in tumor ADC values was found to be significantly increased by 44% at day 4 after therapy (56). The increase in ADC values was correlated with both activation of apoptosis and presentation of cell death within the tumor mass in this study. More recently a study was performed in breast tumor xenografts with applied DW-MRI (9.4T, b-values of 5 and 1000 s/mm^2) to apoptosis-inducing anti-DR5 antibody. In this experimental study performed on nude mice bearing luciferase-positive breast tumors, the effect to increasing doses of treatment was evaluated at different time points. The mean ADC increase was linearly proportional to the mean apoptotic cell density, whereas the tumor volume changes were not different at day 3 after treatment in contrast to the ADC increase. The analysis of the peripheral shell of 1 mm from the outer surface eliminated the ADC increase resulting from central tumor necrosis, improving the specificity of ADC quantification. In this study, DW-MRI as early imaging biomarker for effective apoptosis-induction therapy has been shown in a preclinical breast cancer model (57). Therapeutic efficacy of the apoptosis-inducing strategy was detected as early as 3 days after increased dosing by using ADC quantification at the time when tumor volume changes were not apparent. An improved method of using the ADC data was demonstrated by using analysis of the peripheral shell of the tumor instead of analysis of the entire tumor region. ADC increases in tumor were dose dependant and were persistent with histological markers of apoptosis. The mean ADC increase in tumors was linearly proportional to the mean apoptotic cell density and was inversely proportional to the mean proliferating cell density. Optimizing the time point of imaging after start of treatment is crucial to maximize the accuracy of measuring therapeutic response (57). Based on these data, there is potential in the future to optimize patient therapy on the basis of DW-MRI to monitor effective response at an early interval after initiation of therapy and to prevent unnecessary treatment and establishing individualized therapeutic strategies. This study was performed on a 9.5T MR unit using b-values of 5 and 1000.

Another recently published animal study performed in mice with BT474 breast tumor xenografts analyzed different MRI methods for evaluating the effects of different treatment regimens with tyrosine kinase inhibitor gefitinib (58). Tumor volume, ADC, transendothelial permeability (K^{ps}), and fractional plasma volume (fPV) were measured in three groups receiving (a) control animals for 10 days, or gefitinib as (b) a single daily dose for 10 days or (c) a 2-day pulsed dose. A significant tumor growth delay (pulsed: 439 ± 93; daily: 404 ± 53; controls: 891 ± 174 mm^3; $P < 0.050$) and lower cell density ($P < 0.050$) were observed 9 days after treatment with gefitinib. Tumor ADC increased in treated groups but decreased in controls ($P > 0.050$). Tumor K^{ps} decreased with pulsed treatment at day 4, but increased afterwards, from baseline to day 9 in the daily dose group and decreased in the control group 9 days after therapy. Tumor fPV increased in both treated groups, with a decrease afterwards with pulsed treatment ($P > 0.050$). The authors of this animal study concluded that quantitative MRI can provide sensitive information as to tyrosine kinase inhibitor-induced tumor changes, suggesting the potential of distinguished treatment regimens and ultimately helping in the determination of optimal treatment scheduling for enhancing chemotherapy delivery.

Bone and Soft Tissue Tumors

The response to therapy in bone tumors has been performed by qualitative analysis looking at the signal intensity changes of bone marrow after therapy as well as by quantitative analysis measuring the ADC values. In 24 patients with spine metastases, DW-MRI and spin-echo MRI was performed before and after radiotherapy. Treatment response has been evaluated by qualitative analysis looking at the signal intensity changes of bone marrow after therapy (59). Metastases before radiotherapy showed a hyperintense signal intensity on the images at a b-value of 165 s/mm^2 applied in one direction. A signal decrease 1 month after therapy was defined as response to therapy. In 23 of 24 patients, hypointense signal intensity after successful treatment could be detected, whereas 1 of 24 patients showed persistent hyperintense bone marrow corresponding to no clinical improvement. The authors concluded that DW-MRI allows detecting decreased signal intensity in metastatic disease to the vertebral body marrow corresponding to successful treatment.

In 18 osteogenic and Ewing sarcomas, monitoring of therapeutic response of primary bone tumors has been performed by using DW-MRI. ADC measurements were performed before and 10 to 14 days after finishing chemotherapy. Definitive surgery was performed within 3 days after the postchemotherapy MR study. Necrosis was evaluated on histology. Significantly greater ADC change was observed in the group with tumor necrosis of more than 90% compared with

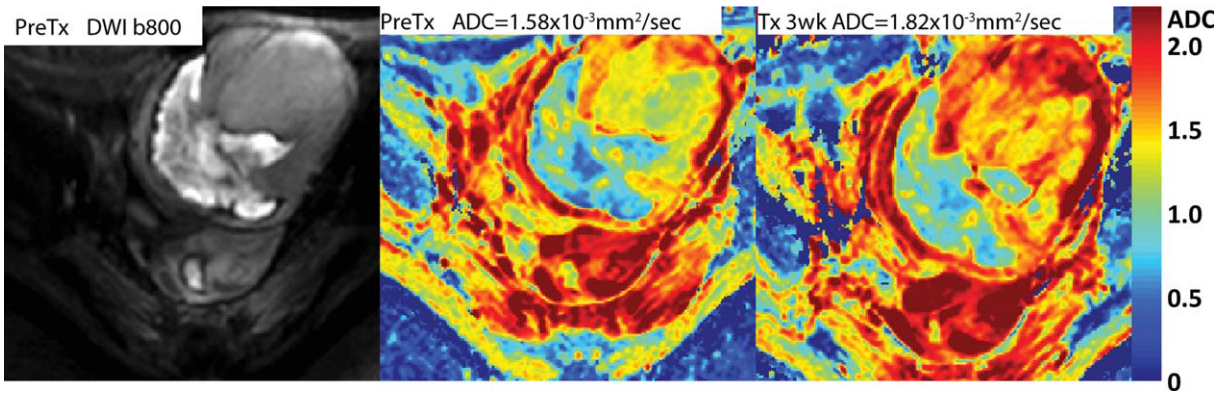

Figure 6. Patient with a soft tissue sarcoma. (Left) Pretreatment high b-value image shows revealing large dense (fibrosis) region on the lower left along with a high cellular region. ADC color overlay maps of the sarcoma (Middle) before and (Right) 3 weeks following chemotherapy. Note that the tumor mass (arrow) exhibited a large increase in tumor ADC values following treatment indicating positive response. (Image kindly provided by T.L. Chenevert, University of Michigan). [Color figure can be viewed in the online issue, which is available at www.interscience.wiley.com.]

the group with less than 90% necrosis on histology after treatment. However, no statistical significant difference in tumor volume between the two groups could be detected. Therefore, the ADC value of DW-MRI could be used as a promising tool for monitoring the therapeutic response to primary bone sarcomas (41). In a preclinical model of metastatic prostate cancer, the fDM as an imaging biomarker for assessing early treatment response has been evaluated to quantify especially distinct therapy-induced changes in the Brownian motion. In contrast to control animals, a significant increase in ADC could already be detected early after treatment. The results of this study have shown the possibility of functional diffusion maps as a biomarker for the detection of bone cancer treatment efficacy with the aim to switch to an alternative therapy in a timelier manner in case of ineffective therapy (60).

These results were confirmed in a patient with metastatic prostate cancer to the bone where DW-MRI was performed at the start of therapy and 2 and 8 weeks after treatment initiation to quantify changes in tumor diffusion values. In all three metastatic lesions that were analyzed, an early increase in diffusion values at 2 weeks which increased further at 8 weeks after treatment initiation could be observed correlating with the decrease in the patients prostate-specific antigen levels suggestive of patient response. Although this has been shown in only one patient, the fDM imaging biomarker may provide a quantifiable therapeutic end point to assess response to patients with metastatic bone cancer (61).

DW-MRI also resulted as useful noninvasive method to monitor anticancer treatment effects in 23 consecutive patients with soft-tissue sarcomas (44). DW-MRI was performed before and after initiation of chemotherapy. A high degree of correlation was found comparing changes in tumor volumes and ADC values ($r = -0.925$; $P < 0.0001$), regardless of the effectiveness of anticancer treatment expressed as changes in tumor volume. As microstructural changes evaluated by DW-MRI are expected to precede change in tumor size and volume, DW-MRI performed at an early stage of fractionated therapy might provide unique prognostic information of effectiveness (44). An example of DW-MRI results obtained following chemotherapy of a patient with a soft tissue sarcoma is shown in Figure 6. In this example, a color ADC map is shown before therapy with a whole tumor average ADC value of 1.58×10^{-3} mm^2/s. At 3 weeks into chemotherapy, the mean ADC value for the sarcoma increased by 15.2% to a value of 1.82×10^{-3} mm^2/s, which is clearly evident from the color overlay maps (see arrows in Fig. 6) indicating a positive response to therapy which was clinically observed for this patient.

Head and Neck Cancer

In head and neck cancer, early evaluation of treatment response may provide prognostic information about treatment efficacy and subsequent tailoring of treatment based on individual response might follow (62). DW-MRI as an imaging biomarker of treatment response of squamous cell head and neck cancer has been evaluated in a mouse model undergoing treatment with chemotherapy, ionizing radiation and combined therapy compared with control animals. The animals were examined during and after treatment for changes in tumor volumes, diffusion values, and survival (63). Radiation therapy had only minimal effect on volumetric growth rate diffusion and survival whereas a combination of chemotherapy and radiotherapy showed an increase in tumor diffusion values which correlated with improved survival. The authors of this animal study concluded that DW-MRI as an imaging biomarker has the potential for early evaluation of the response to chemoradiation treatment in squamous cell carcinoma of the head and neck (63). There is one study performed in 40 patients with newly diagnosed head and neck cancer which performed DW-MRI before, during, and after chemoradiation therapy of head and neck metastases to lymph nodes. In this study, 33 patients with head and neck squamous cell carcinoma and metastatic cervical

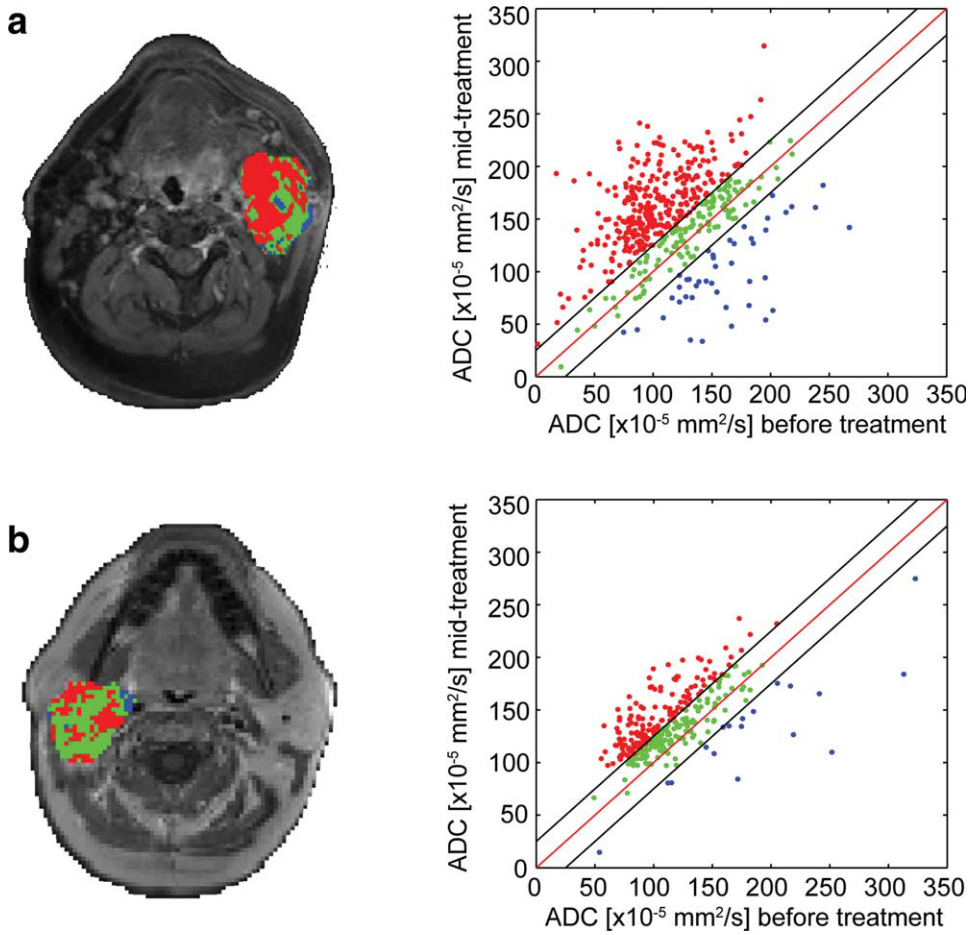

Figure 7. Representative slices of PRM_{ADC} for patients whose conditions were diagnosed as (**A**) complete response (CR) and (**B**) partial response (PR); color-coded volumes of interest are shown as overlays on contrast-enhanced T1-weighted MR images before therapy and corresponding scatter plots for quantification and distribution of ADC before and 3 weeks after treatment initiation for the entire tumor volume. Unity and threshold designating significant change in ADC within the scatter plot are presented by red and black lines, respectively. Voxels with significant increased, decreased, or unchanged ADC values were assigned as red, blue, and green, respectively. Used with permission from Neoplasia Press. Galbán CJ, Mukherji SK, Chenevert TL, et al. Parametric response map analysis of DW-MRI scans of head and neck cancer patients provides for early detection of therapeutic efficacy. Transl Oncol 2009;2:184–190.).

lymph nodes were included and the analysis of ADC values in metastatic lymph nodes were measured before, 1 week after start of chemoradiation therapy, and posttreatment (46). The pretreatment ADC values of complete responders ($1.04 \pm 0.19 \times 10^{-3}$ mm^2/s) were significantly lower than those from partial responders ($1.35 \pm 0.30 \times 10^{-3}$ mm^2/s). In complete responders, significant increase in ADC was observed within 1 week of treatment, which continued until the end of treatment. Furthermore, a significantly larger increase in ADC values was found in complete responders as compared to partial responders by the first week of chemoradiation. The results of this study were quite interesting; however, the ADC values were measured in the metastatic lymph nodes and not on the primary site which would be more challenging and also very helpful for daily decision making in clinical routine. However, the authors of this study concluded that the results suggest that ADC can be used as a marker for prediction and early detection of response to concurrent chemoradiation therapy in head and neck squamous cell carcinoma (46).

In a recent study, PRM_{ADC} was evaluated as an imaging response biomarker in head and neck cancer patients at 3 weeks after initiation of nonsurgical organ preservation therapy (NSOPT) (32). A total of 15 patients were studied in which primary site as well as metastatic lymph nodes were evaluated. Shown in Figure 7 are PRM_{ADC} examples of two different patients who were subsequently found to have different clinical responses to NSOPT. The patient with the most robust therapeutic response exhibited a much larger shift in the overall number of increased ADC voxels at 3 weeks following treatment initiation (Fig. 7A) versus the comparative patient (Fig. 7B). In this study the degree of PRM_{ADC} shift exhibited by individual patients at 3 weeks was found to correlate with tumor control at 6 months. This study reveals the feasibility of using voxel-based assessment of tumor diffusion changes in patients where nonlinear warping

algorithms need to be used for image registration of interval image examinations.

Cervical Cancer

In patients suffering from cervical cancer, DW-MRI has already been performed for treatment monitoring in patients undergoing chemotherapy. In a study of 20 patients suffering from cervical cancer, MRI was performed before treatment, 2 weeks after initiation of radio- and chemotherapy, and at the end of therapy and results were correlated with the change in tumor size in MRI and conventional clinical response (45). In this prospective study performed on a 1.5T MR unit, correlation between change in ADC after 14 days of therapy and tumor size evaluated by conventional MRI was shown. Therefore, DW-MRI has the potential to provide the surrogate marker of treatment response in advanced cervical cancers. The use of ADC offers an early and reproducible indication of tumor response which may ultimately allow the development of individual treatment regimens. Similar results have been described in a study performed in 47 patients with cervical cancer undergoing chemoradiation therapy compared with 26 normal controls. Response to treatment was evaluated if no tumor was visible 3 to 6 months after completion of therapy. In patients with squamous cell carcinomas, the 90th percentile of ADC values was lower in responders than nonresponders ($P < 0.05$). The median ADC in cervix carcinoma was significantly lower compared with normal cervix, whereas the ADC may have predictive value in squamous cell tumors, but further long-term study will determine the ultimate clinical utility of this technique (64).

Rectal Cancer

In rectal cancer, DW-MRI was performed for prediction of response to chemoradiation. Pretreatment ADC values in rectal cancer patients were found to be negatively correlated with response: the presence of higher pretreatment ADC values reflected necrotic tumors that were resistant to therapy (43). The ADC values following treatment were consistently lower than before treatment, which was attributed to possible increase in fibrosis and scar tissue formation in response to treatment. Similar results were observed in another study performed on rectal cancer (64).

CONCLUSION

Changes in tumor volume are currently the clinical response metric used for assessing response of a wide variety of tumor types which must be done late in the time course of treatment. DW-MRI has been shown to be able to detect microstructural changes that precede changes in tumor size. The effects of treatment can be variable: necrosis as potential effect of treatment can be detected as a decrease in perfusion reflecting a decrease in the perfusion fraction (when performing biexponential fitting) as well as an increase in diffusion corresponding to an increase in the true diffusion coefficient. Fibrosis as another potential treatment response can be reflected in a decrease in perfusion (corresponding to decrease in the perfusion fraction Fp) as well as a decrease in diffusion corresponding to an ADC decrease. These findings can also be evaluated by visual analysis of the corresponding high b-value images as well as the ADC map.

For monitoring disease in most tumors and treatment strategies an increased ADC value during treatment corresponds to response, whereas predicting the outcome of response is in most cases correlated with a low pretreatment ADC value showing favorable outcome in most tumors and with most treatment options. However, in rectum carcinoma, a decrease in ADC during treatment corresponded to response due to fibrosis and scar tissue formation. Whereas predicting outcome also depends on the underlying therapy, high pretreatment ADC values have been shown to better correlate with the outcome in tumors treated by vascular targeting agents (65).

DW-MRI has significant potential to be applied as an imaging biomarker of treatment response at an early time interval following treatment initiation. DW-MRI protocols and analyses have to be standardized and need to be tailored to individual tumor types and anatomic sites and therapies. The time point of maximal response has to be evaluated for different tumors and treatment strategies. DW-MRI as ultimate surrogate tumor marker has to be confirmed by comparison to progression-free survival and overall survival. Therefore, multicenter studies to confirm these promising results are warranted.

REFERENCES

1. Therasse P, Arbuck SG, Eisenhauer EA, et al. New guidelines to evaluate the response to treatment in solid tumors. European Organization for Research and Treatment of Cancer, National Cancer Institute of the United States, National Cancer Institute of Canada. J Natl Cancer Inst 2000;92:205–216.
2. Wahl RL, Jacene H, Kasamon Y, Lodge MA. From RECIST to PERCIST: evolving Considerations for PET response criteria in solid tumors. J Nucl Med 2009;50(Suppl 1):122S–150S.
3. Verweij J, Therasse P, Eisenhauer E. Cancer clinical trial outcomes: any progress in tumour-size assessment? Eur J Cancer 2009;45:225–227.
4. Padhani AR, Liu G, Mu-Koh D, et al. Diffusion-weighted magnetic resonance imaging as a cancer biomarker: consensus and recommendations. Neoplasia 2009;11:102–125.
5. Griswold MA, Jakob PM, Heidemann RM, et al. Generalized autocalibrating partially parallel acquisitions (GRAPPA). Magn Reson Med 2002;47:1202–1210.
6. Pruessmann KP, Weiger M, Scheidegger MB, Boesiger P. SENSE: sensitivity encoding for fast MRI. Magn Reson Med 1999;42: 952–962.
7. Sodickson DK, Griswold MA, Jakob PM. SMASH imaging. Magn Reson Imaging Clin N Am 1999;7:237–254, vii–viii.
8. Ivancevic MK, Kwee TC, Takahara T, et al. Diffusion-weighted MR imaging of the liver at 3.0 Tesla using TRacking Only Navigator echo (TRON): a feasibility study. J Magn Reson Imaging 2009;30: 1027–1033.
9. Kwee TC, Takahara T, Koh DM, Nievelstein RA, Luijten PR. Comparison and reproducibility of ADC measurements in breathhold, respiratory triggered, and free-breathing diffusion-weighted MR imaging of the liver. J Magn Reson Imaging 2008;28:1141–1148.
10. Nakayama T, Yoshida S, Fujii Y, et al. [Use of diffusion-weighted MRI in monitoring response of lymph node metastatic bladder cancer treated with chemotherary]. Nippon Hinyokika Gakkai Zasshi 2008;99:737–741.

11. Hardy PA, Recht MP, Piraino DW. Fat suppressed MRI of articular cartilage with a spatial-spectral excitation pulse. J Magn Reson Imaging 1998;8:1279–1287.
12. Bydder GM, Hajnal JV, Young IR. MRI: use of the inversion recovery pulse sequence. Clin Radiol 1998;53:159–176.
13. Kuroda K, Oshio K, Mulkern RV, Jolesz FA. Optimization of chemical shift selective suppression of fat. Magn Reson Med 1998;40:505–510.
14. Clark CA, Le Bihan D. Water diffusion compartmentation and anisotropy at high b values in the human brain. Magn Reson Med 2000;44:852–859.
15. Tofts PS, Lloyd D, Clark CA, et al. Test liquids for quantitative MRI measurements of self-diffusion coefficient in vivo. Magn Reson Med 2000;43:368–374.
16. Delakis I, Moore EM, Leach MO, De Wilde JP. Developing a quality control protocol for diffusion imaging on a clinical MRI system. Phys Med Biol 2004;49:1409–1422.
17. Chenevert TL, McKeever PE, Ross BD. Monitoring early response of experimental brain tumors to therapy using diffusion magnetic resonance imaging. Clin Cancer Res 1997;3:1457–1466.
18. Chenevert TL, Stegman LD, Taylor JM, et al. Diffusion magnetic resonance imaging: an early surrogate marker of therapeutic efficacy in brain tumors. J Natl Cancer Inst 2000;92:2029–2036.
19. Ross BD, Chenevert TL, Kim B, Ben-Yoseph O. Magnetic resonance imaging and spectroscopy: application to experimental neuro-oncology. Q Magn Reson Biol Med 1994:89–106.
20. Zhao M, Pipe JG, Bonnett J, Evelhoch JL. Early detection of treatment response by diffusion-weighted 1H-NMR spectroscopy in a murine tumour in vivo. Br J Cancer 1996;73:61–64.
21. Poptani H, Puumalainen AM, Grohn OH, et al. Monitoring thymidine kinase and ganciclovir-induced changes in rat malignant glioma in vivo by nuclear magnetic resonance imaging. Cancer Gene Ther 1998;5:101–109.
22. Moffat BA, Hall DE, Stojanovska J, et al. Diffusion imaging for evaluation of tumor therapies in preclinical animal models. MAGMA 2004;17:249–259.
23. Galons JP, Altbach MI, Paine-Murrieta GD, Taylor CW, Gillies RJ. Early increases in breast tumor xenograft water mobility in response to paclitaxel therapy detected by non-invasive diffusion magnetic resonance imaging. Neoplasia 1999;1:113–117.
24. Hall DE, Moffat BA, Stojanovska J, et al. Therapeutic efficacy of DTI-015 using diffusion magnetic resonance imaging as an early surrogate marker. Clin Cancer Res 2004;10:7852–7859.
25. Chinnaiyan AM, Prasad U, Shankar S, et al. Combined effect of tumor necrosis factor-related apoptosis-inducing ligand and ionizing radiation in breast cancer therapy. Proc Natl Acad Sci U S A 2000;97:1754–1759.
26. Hamstra DA, Lee KC, Tychewicz JM, et al. The use of 19F spectroscopy and diffusion-weighted MRI to evaluate differences in gene-dependent enzyme prodrug therapies. Mol Ther 2004;10: 916–928.
27. Stegman LD, Rehemtulla A, Hamstra DA, et al. Diffusion MRI detects early events in the response of a glioma model to the yeast cytosine deaminase gene therapy strategy. Gene Ther 2000; 7:1005–1010.
28. Theilmann RJ, Borders R, Trouard TP, et al. Changes in water mobility measured by diffusion MRI predict response of metastatic breast cancer to chemotherapy. Neoplasia 2004;6:831–837.
29. Schepkin VD, Lee KC, Kuszpit K, et al. Proton and sodium MRI assessment of emerging tumor chemotherapeutic resistance. NMR Biomed 2006;19:1035–1042.
30. Larocque MP, Syme A, Yahya A, Wachowicz K, Allalunis-Turner J, Fallone BG. Temporal and dose dependence of T2 and ADC at 9.4 T in a mouse model following single fraction radiation therapy. Med Phys 2009;36:2948–2954.
31. Moffat BA, Chenevert TL, Lawrence TS, et al. Functional diffusion map: a noninvasive MRI biomarker for early stratification of clinical brain tumor response. Proc Natl Acad Sci U S A 2005;102: 5524–5529.
32. Galbán CJ, Mukherji SK, Chenevert TL, et al. Parametric response map analysis of DW-MRI scans of head and neck cancer patients provides for early detection of therapeutic efficacy. Transl Oncol 2009;2:184–190.
33. Moffat BA, Chenevert TL, Meyer CR, et al. The functional diffusion map: an imaging biomarker for the early prediction of cancer treatment outcome. Neoplasia 2006;8:259–267.
34. Hamstra DA, Chenevert TL, Moffat BA, et al. Evaluation of the functional diffusion map as an early biomarker of time-to-progression and overall survival in high-grade glioma. Proc Natl Acad Sci U S A 2005;102:16759–16764.
35. Hamstra DA, Galban CJ, Meyer CR, et al. Functional diffusion map as an early imaging biomarker for high-grade glioma: correlation with conventional radiologic response and overall survival. J Clin Oncol 2008;26:3387–3394.
36. Galban CJ, Chenevert TL, Meyer CR, et al. The parametric response map is an imaging biomarker for early cancer treatment outcome. Nat Med 2009;15:572–576.
37. Le Bihan D, Breton E, Lallemand D, Aubin ML, Vignaud J, Laval-Jeantet M. Separation of diffusion and perfusion in intravoxel incoherent motion MR imaging. Radiology 1988;168:497–505.
38. Thoeny HC, De Keyzer F, Chen F, et al. Diffusion-weighted MR imaging in monitoring the effect of a vascular targeting agent on rhabdomyosarcoma in rats. Radiology 2005;234:756–764.
39. Thoeny HC, De Keyzer F, Vandecaveye V, et al. Effect of vascular targeting agent in rat tumor model: dynamic contrast-enhanced versus diffusion-weighted MR imaging. Radiology 2005;237:492–499.
40. Le Bihan D. Intravoxel incoherent motion perfusion MR imaging: a wake-up call. Radiology 2008;249:748–752.
41. Hayashida Y, Yakushiji T, Awai K, et al. Monitoring therapeutic responses of primary bone tumors by diffusion-weighted image: initial results. Eur Radiol 2006;16:2637–2643.
42. Sharma U, Danishad KK, Seenu V, Jagannathan NR. Longitudinal study of the assessment by MRI and diffusion-weighted imaging of tumor response in patients with locally advanced breast cancer undergoing neoadjuvant chemotherapy. NMR Biomed 2009;22:104–113.
43. Dzik-Jurasz A, Domenig C, George M, et al. Diffusion MRI for prediction of response of rectal cancer to chemoradiation. Lancet 2002;360:307–308.
44. Dudeck O, Zeile M, Pink D, et al. Diffusion-weighted magnetic resonance imaging allows monitoring of anticancer treatment effects in patients with soft-tissue sarcomas. J Magn Reson Imaging 2008;27:1109–1113.
45. Harry VN, Semple SI, Gilbert FJ, Parkin DE. Diffusion-weighted magnetic resonance imaging in the early detection of response to chemoradiation in cervical cancer. Gynecol Oncol 2008;111:213–220.
46. Kim S, Loevner L, Quon H, et al. Diffusion-weighted magnetic resonance imaging for predicting and detecting early response to chemoradiation therapy of squamous cell carcinomas of the head and neck. Clin Cancer Res 2009;15:986–994.
47. Koh DM, Scurr E, Collins D, et al. Predicting response of colorectal hepatic metastasis: value of pretreatment apparent diffusion coefficients. AJR Am J Roentgenol 2007;188:1001–1008.
48. Cui Y, Zhang XP, Sun YS, Tang L, Shen L. Apparent diffusion coefficient: potential imaging biomarker for prediction and early detection of response to chemotherapy in hepatic metastases. Radiology 2008;248:894–900.
49. Marugami N, Tanaka T, Kitano S, et al. Early detection of therapeutic response to hepatic arterial infusion chemotherapy of liver metastases from colorectal cancer using diffusion-weighted MR imaging. Cardiovasc Intervent Radiol 2009;32:638–646.
50. Schraml C, Schwenzer NF, Clasen S, et al. Navigator respiratory-triggered diffusion-weighted imaging in the follow-up after hepatic radiofrequency ablation-initial results. J Magn Reson Imaging 2009;29:1308–1316.
51. Kamel IR, Liapi E, Reyes DK, Zahurak M, Bluemke DA, Geschwind JF. Unresectable hepatocellular carcinoma: serial early vascular and cellular changes after transarterial chemoembolization as detected with MR imaging. Radiology 2009;250:466–473.
52. Yu JS, Kim JH, Chung JJ, Kim KW. Added value of diffusion-weighted imaging in the MRI assessment of perilesional tumor recurrence after chemoembolization of hepatocellular carcinomas. J Magn Reson Imaging 2009;30:153–160.
53. Niwa T, Ueno M, Ohkawa S, et al. Advanced pancreatic cancer: the use of the apparent diffusion coefficient to predict response to chemotherapy. Br J Radiol 2009;82:28–34.
54. Kremser C, Judmaier W, Hein P, Griebel J, Lukas P, de Vries A. Preliminary results on the influence of chemoradiation on apparent diffusion coefficients of primary rectal carcinoma measured by magnetic resonance imaging. Strahlenther Onkol 2003;179:641–649.
55. Pickles MD, Gibbs P, Lowry M, Turnbull LW. Diffusion changes precede size reduction in neoadjuvant treatment of breast cancer. Magn Reson Imaging 2006;24:843–847.

56. Lee KC, Moffat BA, Schott AF, et al. Prospective early response imaging biomarker for neoadjuvant breast cancer chemotherapy. Clin Cancer Res 2007;13:443–450.
57. Kim H, Morgan DE, Zeng H, et al. Breast tumor xenografts: diffusion-weighted MR imaging to assess early therapy with novel apoptosis-inducing anti-DR5 antibody. Radiology 2008;248: 844–851.
58. Aliu SO, Wilmes LJ, Moasser MM, et al. MRI methods for evaluating the effects of tyrosine kinase inhibitor administration used to enhance chemotherapy efficiency in a breast tumor xenograft model. J Magn Reson Imaging 2009;29:1071–1079.
59. Byun WM, Shin SO, Chang Y, Lee SJ, Finsterbusch J, Frahm J. Diffusion-weighted MR imaging of metastatic disease of the spine: assessment of response to therapy. AJNR Am J Neuroradiol 2002;23:906–912.
60. Lee KC, Sud S, Meyer CR, et al. An imaging biomarker of early treatment response in prostate cancer that has metastasized to the bone. Cancer Res 2007;67:3524–3528.
61. Lee KC, Bradley DA, Hussain M, et al. A feasibility study evaluating the functional diffusion map as a predictive imaging biomarker for detection of treatment response in a patient with metastatic prostate cancer to the bone. Neoplasia 2007;9: 1003–1011.
62. Forastiere AA, Ang K, Brizel D, et al. Head and neck cancers. J Natl Compr Canc Netw 2005;3:316–391.
63. Hamstra DA, Lee KC, Moffat BA, Chenevert TL, Rehemtulla A, Ross BD. Diffusion magnetic resonance imaging: an imaging treatment response biomarker to chemoradiotherapy in a mouse model of squamous cell cancer of the head and neck. Transl Oncol 2008;1:187–194.
64. McVeigh PZ, Syed AM, Milosevic M, Fyles A, Haider MA. Diffusion-weighted MRI in cervical cancer. Eur Radiol 2008;18:1058–1064.
65. Thoeny HC, De Keyzer F, Chen F, et al. Diffusion-weighted magnetic resonance imaging allows noninvasive in vivo monitoring of the effects of combretastatin a-4 phosphate after repeated administration. Neoplasia 2005;7:779–787.